The Meteoritical Society

Meteoritics & Planetary Science 53, Nr 12, 2541–2557 (2018)
doi: 10.1111/maps.13174

From the mid-Ordovician into the Late Silurian: Changes in the micrometeorite flux after the L chondrite parent breakup

Ellinor MARTIN[1], Birger SCHMITZ[1*], and Hans-Peter SCHÖNLAUB[2]

[1]Astrogeobiology Laboratory, Department of Physics, Lund University, Box 118, SE-221 00 Lund, Sweden
[2]Center for Geosciences, Austrian Academy of Sciences, Dr. Ignaz Seipel-Platz 2, A-1010 Vienna, Austria
[*]Corresponding author. E-mail: birger.schmitz@nuclear.lu.se

(Received 10 January 2018; revision accepted 29 May 2018)

Abstract–We present the first reconstruction of the micrometeorite flux to Earth in the Silurian Period. We searched 321 kg of condensed, marine limestone from the Late Silurian Cellon section, southern Austria, for refractory chrome-spinel grains from micrometeorites that fell on the ancient sea floor. A total of 155 extraterrestrial spinel grains (10 grains >63 μm, and 145 in the 32–63 μm fraction) were recovered. For comparison, we searched 102 kg of similar limestone from the mid-Ordovician Komstad Formation in southern Sweden. This limestone formed within ~1 Ma after the breakup of the L chondrite parent body (LCPB) in the asteroid belt. In the sample we found 444 extraterrestrial spinel grains in the >63 μm fraction, and estimate a content of at least 7000 such grains in the 32–63 μm fraction. Our results show that in the late Silurian, ~40 Ma after the LCPB, the flux of ordinary equilibrated chondrites has decreased by two orders of magnitude, almost down to background levels. Among the ordinary chondrites, the dominance of L-chondritic micrometeorites has waned off significantly, from >99% in the post-LCPB mid-Ordovician to ~60% in the Late Silurian, with ~30% H-, and ~10% LL-chondritic grains. In the Late Silurian, primitive achondrite abundances are similar to today's value, contrasting to the much higher abundances observed in pre-LCPB mid-Ordovician sediments.

INTRODUCTION

Earth's geological record has given us some insights into the history of the asteroid belt and the solar system at large, but interpreting the record is challenging. For example, the Earth's impact crater record, with 190 confirmed impact structures as of today (Earth Impact Database 2017), is heavily affected by erosional processes and is biased toward larger craters as small craters quickly erode in just a few million years (e.g., Koeberl 2002). The impact structures on the Moon give us an indication of the rate of impacts and what the surface of the Earth would look like with the absence of plate tectonics, large oceans, and erosional processes (McEwen et al. 1997; Kirchoff et al. 2013). As for the late evolution of the asteroid belt, astronomers have used backtracking of asteroid family members and their spread in semimajor axis to determine when different asteroid families formed through collisional events (e.g., Vokrouhlický et al. 2006; Spoto et al. 2015). Sophisticated models have been used to relate these collisional events to the delivery of meteorites to Earth (Bottke et al. 2005).

A more recent information source with regard to the late history of the solar system and the asteroid belt is Earth's sedimentary record (e.g., Farley et al. 2006; Schmitz 2013). This record holds clues to the dynamics and evolution of the solar system, mainly the asteroid belt; information that can be related also to changes here on Earth. Disruptions of large asteroids and subsequent heightened flux of cosmic dust can be located in the sedimentary record by searches for enrichments of ^{3}He retained in interplanetary dust particles (typically <30 μm), or refractory spinel grains (>30 μm) from micrometeorites that decomposed on ancient sea floors. For example, a ^{3}He anomaly in late Miocene sediments in Italy has been related to the formation of the Veritas family in the asteroid belt about 8 Ma ago (Farley et al. 2006). The Veritas family, however, is not situated well in the asteroid belt

for any larger particles to become Earth crossing. Extraterrestrial spinels have been used to locate a level in Earth's mid-Ordovician sedimentary strata where the first dust reaches Earth from the breakup of the 100–150 km in diameter L chondrite parent body (LCPB) (Schmitz et al. 2003; Schmitz 2013). This event, about 466 Ma ago, is the largest documented breakup event in late solar-history time (Haack et al. 1996). The abundance of sediment-dispersed spinels from this event indicates a two orders of magnitude increase in the flux of extraterrestrial matter to Earth following the breakup. More than 100 fossil L-chondritic meteorites (1–21 cm large) have been found in coeval marine limestone strata, providing additional support for the link to the LCPB (Schmitz et al. 2001; Bridges et al. 2007; Schmitz 2013). The LCPB has been linked to the formation of the Gefion family, a large cluster of asteroids located close to the 5:2 Jupiter resonance, a powerful resonance capable of ejecting material into the inner solar system on a relatively short time scale, like the ones detected in the cosmic ray exposure ages of the fossil meteorites (Nesvorný et al. 2009).

Extraterrestrial chrome-rich spinels from ancient marine sediments have now successfully been used as a proxy for the flux of extraterrestrial matter to Earth for a few "windows" in deep time other than immediately after the LCPB. Reconstructions of the micrometeorite flux using spinels have been performed for the late Eocene (Boschi et al. 2017), the Early Cretaceous (Schmitz et al. 2017), and the mid-Ordovician pre-LCPB (Heck et al. 2017). Noble-gas isotopic measurements of sediment-dispersed extraterrestrial Cr-spinel grains show high concentrations of solar wind implanted gases, indicating that the grains represent residues of micrometeorites, as solar wind can only penetrate the outermost ~100 nanometers of an object in space (Heck et al. 2008; Meier et al. 2010, 2014). Therefore, the flux estimates in this paper relate to micrometeorites. The chrome-spinel grains endure both weathering, diagenesis, and the harsh chemical treatments used to recover them, and they generally retain their chemical and isotopic properties related to their origin (e.g., Schmitz 2013; Heck et al. 2017). In the present study, we add the Late Silurian to the time windows studied for micrometeorites. We are interested in how the flux of micrometeorites to Earth had evolved 40 Ma after the LCPB. In the Cellon section in Austria a Late Silurian, condensed limestone variety, known as the "Orthoceras limestone," is exposed (Corradini et al. 2014). This type of limestone is very similar to the condensed mid-Ordovician "Orthoceratite limestone" in Sweden, which has yielded the abundant fossil meteorites and micrometeoritic spinel grains from the LCPB. By recovering the Cr-spinels from 100 kg sized samples of well age-defined limestone both from a micrometeorite-rich level in the mid-Ordovician and three levels in the Late Silurian, we aim to see how the flux of L-chondritic material has evolved by the Late Silurian. The two types of limestones have similar estimated mean sedimentation rates (2–4 mm per ka), which make a confident flux comparison between the two sections possible. For the mid-Ordovician we focus on a 100 kg large sample from a thin bed that in a study by Häggström and Schmitz (2007) was shown to be particularly deficient in terrestrial spinels, as abundant terrestrial spinels in a sample tend to "dilute" and obscure co-occurring extraterrestrial grains. One aim with a large sample from this bed is to test if the abundant post-LCPB L-chondritic grains are accompanied by any grains from the asteroid that disrupted the L chondrite parent body. The only mid-Ordovician fossil meteorite that is not an L chondrite appears to be a kind of primitive achondrite that does not fall on Earth today (Schmitz et al. 2016). This meteorite has been proposed to be a fragment of the impactor asteroid. Last, it has been argued that following the LCPB, secondary collisions on the Moon could eject lunar meteorites in space (Artemieva and Shuvalov 2008), and we test this by searching for lunar spinel grains in the mid-Ordovician sample.

GEOLOGICAL SETTING

Cellon Section

The Cellon section is the stratotype section for Silurian rocks in the Southern Alps (Fig. 1). It is located in the Central Carnic Alps that stretches across the Italian/Austrian border for more than 140 km (Brett et al. 2009; Histon 2012; Corradini et al. 2014) continuing to the east into the Western Karawanke Mountains in northern Slovenia. The strata range from the Upper Ordovician to the Lower Carboniferous and represent the so-called Plöcken facies formed as a shallow to relatively deep marine carbonate sequence. Since the pioneering work by Geyer (1894), many geological studies have been carried out in the Cellon section, and Walliser (1964) laid the biostratigraphic framework upon which proceeding paleontological studies are based (Brett et al. [2009] and references therein). More than 40 m of Silurian "Orthoceras limestone" crop out here, spanning the interval from the Late Llandovery to the Přídolí. The term "Orthoceras limestone" is an informal facies description. The "Orthoceras limestone" in the Cellon section varies in color from black to red reflecting deposition under oxic to anoxic conditions. The Silurian part of the section consists of the following lithological units, in ascending

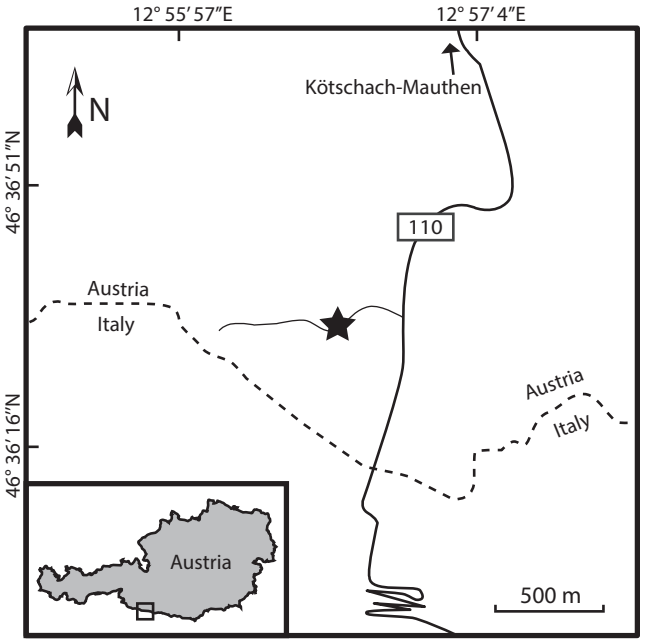

Fig. 1. Map showing the location of the Cellon section (star).

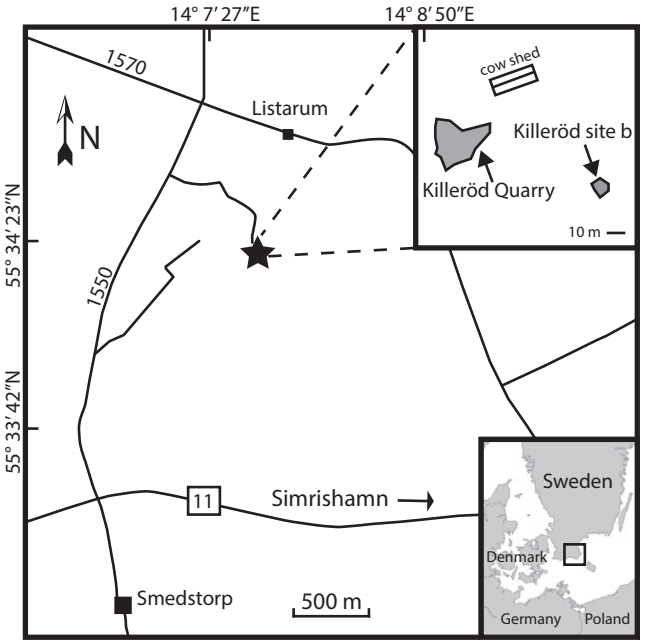

Fig. 2. Map showing the location of the two Killeröd quarries at the Killeröd site (star).

order: Kok (beds 9–19), Cardiola (beds 20–24A), Alticola (beds 25–39A), and Megaerella (beds 40–47B) formations. Bed numbers are from Walliser (1964). The Kok Formation covers the Llandovery to lower Ludlow and is around 13.5 m thick. The lower portion (beds 9–15) is composed of shales and ferruginous limestones. The upper part, from beds 16–19, contains a reddish, wavy-bedded massive wackestone with abundant orthoconic nautiloids and many other fossils. The overlying Cardiola Formation consists of dark-gray-black limestone alternating with black shales comprising only ~3.5 m (beds 20–24A). The Alticola Formation is a gray to reddish nautiloid-bearing limestone ranging from Ludlow to Pridolí (beds 25–39A). The thickness is around 20 m. The Megaerella Formation is of Prídolí to lowermost Lochkovian age and consists of 8 m of massive wackestone to packstone with a shallowing upward trend (Brett et al. 2009; Corradini et al. 2014).

The depositional environment during Llandovery and Wenlock was moderately shallow with episodic deepening (condensed sequences) forming the lower parts of the Kok Formation and deepening toward the upper part (middle Ludlow), transitioning into the Cardiola Formation, representing a deeper offshore setting with periods of nondeposition. A more stable pelagic setting is developed in the Alticola and Megaerella formations (Upper Ludlow and Lower Prídolí) (Histon and Schönlaub 1999; Schönlaub and Histon 2000; Histon 2012). Overall, the succession represents a transgressive regime from Llandovery to Ludlow, where Ludlow-aged strata mostly consist of condensed pelagic limestone deposited at a slow sedimentation rate with periods of highstands represented by dark organic-rich shale layers (Brett et al. 2009). Cephalopod-rich nodular to massive carbonates overlay these highstand intervals, which indicate condensed offshore facies (Histon 2012).

The average sedimentation rate for both the Kok and Alticola formations studied here is ~4 mm per ka based on the thicknesses of the intervals corresponding to the Ludfordian and Gorstian ages (~17.5 m corresponding to ~4.4 Ma) from the international chronostratigraphic chart (Walliser 1964; Cohen et al. 2013).

Killeröd Section

The Killeröd section is located in southeast Scania, Sweden, around 13 km west of the town Simrishamn in two abandoned quarries (Fig. 2). The section is proposed as the paratype section of the mid-Ordovician Komstad Limestone, as the type section in the Komstad quarries, 1 km west of Killeröd, is largely inaccessible (Nielsen 1995). The limestone is a dark, organic-rich wackestone/packstone that was deposited in an epicontinental sea that covered a large part of Baltoscandia through much of the early Paleozoic. In the limestone sequence there are also intercepting layers of lighter colored marly limestone with thinner clay-rich bands. The thickness of the Komstad Limestone in the Killeröd area is estimated to a minimum of 15 m (Nielsen 1995) and spans the Volkhov and Kunda

Baltoscandian stages in the Darriwillian global stage. The sediment was deposited far from any coast and is very condensed, having formed at 2–4 mm per ka. The Komstad limestone is a variety of the "Orthoceratite Limestone," the dominating sediment type over large parts of Baltoscandia during this period. Over much of its geographic range, the Orthoceratite Limestone is a reddish, condensed limestone, rich in fossil nautiloid conchs. The limestone is characterized by abundant hardground surfaces, representing periods of nondeposition. It is the Orthoceratite Limestone that has yielded more than 100 fossil meteorites at Kinnekulle 350 km north of Killeröd (Schmitz et al. 1997, 2001; Schmitz 2013). The depth at which the Orthoceratite Limestone formed has been intensively debated with some authors arguing for "deep" conditions (one to several hundred meters) (Lindström 1963; Chen and Lindström 1991). Others argue that depths were less than 100 m (e.g., Jaanusson 1973; Nielsen 1995; Lindskog 2014). Some of the confusion may reflect that authors base their generalizations on different sections that represent different depth regimes. The Baltica continent was situated at around 30° south of the paleo-equator during the Middle Ordovician and was slowly drifting north (Torsvik et al. 1992; Cocks and Torsvik 2005).

Häggström and Schmitz (2007) studied 13 samples weighing between 14 and 28 kg across the mid-Ordovician limestone exposed in the Killeröd area. They showed that the stratigraphic distribution of extraterrestrial spinels was similar to that in the Hällekis section, 350 km to the north. In the lower part of the section, corresponding to the trilobite zones *Megistaspis simon* and *M. limbata*, and the lower part of the *Asaphus expansus* zone, they found one H-chondritic and one L-chondritic grain (>63 μm) in 125 kg of limestone, whereas from the upper part of the *A. expansus* zone and into the *A. raniceps* zone concentrations of the L-chondritic grains rapidly increase by two orders of magnitude following the LCPB. This trend has later been confirmed also in mid-Ordovician sections in China and western Russia (Cronholm and Schmitz 2010; Lindskog et al. 2012). In their study of the Komstad Limestone, Häggström and Schmitz (2007) located a bed particularly rich in L-chondritic grains (>63 μm), 4.5 grains kg^{-1}, compared to generally about 2 such grains kg^{-1} in typical post-LCPB Orthoceratite Limestone in Sweden. This bed, which is the focus of the present study, probably formed a factor of two slower than equivalent beds from other sections, during a 10–20 ka period with very stable sea floor conditions and absence of volcanism, tectonism, or sea-level variations. Terrestrial Cr-spinels are generally very rare in the Komstad Limestone, but one bed immediately above the bed studied here contains as much as 2.4 such grains per kilogram rock.

MATERIALS AND METHODS

Samples

The Cellon section is exposed just north of the Austrian/Italian border next to highway 110 (Plöckenpass Strasse), along the eastern side of Mount Cellon at coordinates 46°36′32″N, 12°56′31″E (Fig. 1). The succession crops out in a narrow avalanche gorge at an altitude of around 1500 m above sea level. The closest city is Kötschach-Mauthen about 8 km to the NNE. The Silurian samples, each between 103 and 109 kg large (321 kg in total), were extracted from three beds in the Cellon section. All samples are within the Ludlow Series. The lowest sample (S-24), with a blackish gray color, is from the Kok Formation (Gorstian age), bed 18A, in the *A. ploeckensis* Conodont zone. The second sample (S-29) is within the Alticola Formation (Ludfordian age), in bed 25B with a light-gray color. The uppermost sample (S-30) is also located within the Alticola Formation in a bed between beds 26B and 27, a 25 cm thick level exceptionally rich in nautiloid conchs and with a pinkish dark-gray color. The latter two samples are within the *Pedavis latialata—Ozarkodina snajdri* Interval zone (Corradini et al. 2014; fig. 3).

The mid-Ordovician sample (Kom-9.71) was extracted from the Komstad Limestone Formation in the Killeröd area (Fig. 2). The sampling area for this study is the smaller water-filled quarry ~60 m from the main Killeröd quarry, denoted Killeröd "site b" by Nielsen (1995) with coordinates 55°34′20.95″N, 14°7′54.72″E. At Killeröd site b, the thickness of the exposed section measures about 4 m from the small hill down to the water level. The outcrop of the section at site b comprises the transition between the *Asaphus expansus* and *Asaphus raniceps* trilobite zones. The limestone sample of 102 kg was recovered from a thin, ~12 cm, interval of the Komstad Limestone Formation in the upper *A. expansus* trilobite zone, within level +35 in Nielsen (1995) and from levels 9.71–9.84 m in Häggström and Schmitz (2007). This is the interval particularly rich in extraterrestrial spinels and with a very low content of terrestrial spinels, making it ideal for reconstructions of the ancient micrometeorite flux. The base of the level is located ~50 cm below the base of the *A. raniceps* trilobite zone. The sampled bed is easily recognized in the field, located on a ledge on top of the smaller quarry at the northwestern side. The bed is rich in large nautiloid conchs and some macroscopic trilobites.

Separation of Cr-Spinels and Chemical Analyses

The limestone samples were handled in the Astrogeobiology Laboratory, specially built for the separation of microscopic spinels from large limestone samples (see www.astrogeobiology.org). Samples were thoroughly cleaned before being dissolved in 500 L barrels with 6 M hydrochloric acid. The clay-rich residue was neutralized and sieved through a 32 μm meshed sieve to remove the clay fraction. In order to remove silicates, the residue was placed in 11 M hydrofluoric acid at room temperature for about 3 days with occasional stirring. If needed, samples were also density separated with LST Heavy Liquid (lithium heteropolytungstate). Samples were again sieved and separated into fractions 32–63 μm and 63–355 μm. The samples were then transferred to Petri dishes, searched for opaque mineral grains that were picked with a fine brush under a stereomicroscope and moved to carbon tape. In the Silurian samples, we picked grains in both the 32–63 μm and 63–355 μm fractions, whereas in the Ordovician sample, because of the extreme abundance of extraterrestrial spinels, we only used the 63–355 μm fraction.

A preliminary chemical analysis of the grains on carbon tape was made with an Oxford Instruments INCA X-Sight energy-dispersive spectrometer (EDS) attached to a Hitachi S-3400N scanning electron microscope (SEM). Cobalt is used as a standard, and we used an acceleration voltage of 15 kV with 30 s counting live-time. Grains containing chromium were then molded in epoxy resin and polished with 1 μm diamond paste and coated with carbon. Qualitative element analysis was then performed on the polished grains with 80 s counting live-time in at least three spots with SEM/EDS. Spots for analysis were selected away from fractures or diagenetically altered parts of the grain. An image was taken of each grain and added to a spreadsheet together with information of chemistry for future references.

Division of Grains and Definitions

Grains from equilibrated ordinary chondrites (EC) can easily be identified due to very narrow ranges in elemental composition (Schmitz 2013). The ranges used here in oxide weight percentage are: Cr_2O_3 ~55–60 wt%, FeO ~25–30 wt%, Al_2O_3 ~5–8 wt%, MgO ~1.5–4.0 wt%, V_2O_3 ~0.6–0.9 wt%, TiO_2 ~1.4–4.5 wt% (from Schmitz 2013; with a revised upper limit for TiO_2; see Table S1 in supporting information for details). If one or two oxides have values significantly outside the ranges that define EC grains, but the grains still likely are chondritic based on the context, we define them here in a subcategory called Outlier EC grains. Most or all of these grains are EC grains that have been diagenetically altered, and are excluded from the EC statistics.

The EC grains can additionally be divided into groups H, L, and LL based on oxygen isotopic ratios and TiO_2 content (Heck et al. 2016; Schmitz et al. 2017). Our previous studies have shown that the isotopic and elemental approaches give about the same results. Here we apply solely TiO_2 for the division using the same ranges as in previous studies: H $\leq$2.50 wt%, L 2.51–3.39 wt%, and LL $\geq$3.40 wt%. The method of determining the three groups of equilibrated ordinary chondrites using TiO_2 is based first on the stability of titanium dioxide, which is the oxide most resistant to diagenetic alteration. Second, the TiO_2 values of each group follow an approximate Gaussian distribution with distinctive averages that separate them (see fig. 4 in Heck et al. 2016). The averages of H, L, and LL are 2.2, 2.7, and 3.4 wt%, respectively. The limits of the TiO_2 ranges are set arbitrarily but have to be used consistently when comparing the micrometeorite flux in different time slices (Schmitz et al. 2017). The caveat of the method is that the TiO_2 values for each group overlap slightly with each other, which can bias the results, particularly when one of the groups dominates over the others. Also the $\Delta^{17}O$ values overlap between the three groups, and for the L and LL groups, the overlap is even more pronounced than with TiO_2 (see Heck et al. [2016] for further discussions). We use here two ways of dividing grains by their TiO_2 content. In the first approach we rely entirely on TiO_2 content in relation to the ranges set. In the second approach we correct the percentages obtained in the first approach by assuming that 10% of the grains belonging to a particular group lies in the tails that extend into the "neighbor" groups. The use of the value 10% is based on the results from the combined oxygen isotopic and TiO_2 analyses of 119 EC grains from mid-Ordovician post-LCPB beds in Heck et al. (2016).

The grains that do not fall in the EC or Outlier EC categories are defined as "other chrome-spinel with V_2O_3 $\geq$0.45 wt%" (OC-V), or "all other chrome-rich spinel" (OC) (Schmitz and Häggström 2006; Schmitz et al. 2017). A high content of vanadium (>0.5 wt% V_2O_3) is much more common in extraterrestrial than in terrestrial spinels. An OC-V grain is likely of extraterrestrial origin, but can in rare cases be terrestrial, whereas an OC grain likely is terrestrial, but can be extraterrestrial. Oxygen isotopic analysis is needed to firmly establish the origins of OC and OC-V grains. Some clues about the origin of these grains can also be obtained from their relative abundances. In an assemblage very rich in EC grains and with some OC-V grains, but only rare OC grains, the likelihood is high

that also the OC-V and OC grains are extraterrestrial. Knowledge about the type of local bedrock that potentially can provide terrestrial grains can also be helpful in interpreting the origin of the spinel grains. OC grains are plotted with compositional fields of common terrestrial spinels from Barnes and Roeder (2001) using molar ratios of Cr/Cr+Al (Cr#), Fe^{2+}/Mg+Fe^{2+} (Fe#), and Fe^{3+}/Cr+Al+Fe^{3+} (Fe/3+#), and weight percentage of TiO_2, as these can give an indication of provenance. As a reference, spinels from ordinary equilibrated chondrites have (on average) narrow high ratios of Cr# and Fe# (~0.8–0.9) (Wlotzka 2005) and very low Fe/3+# (<0.05) (Roeder 1994).

RESULTS

An overview comparing the micrometeorite flux in the mid-Ordovician and the Silurian is given in Fig. 3. The most important result is the two orders of magnitude decrease in micrometeorite flux from the post-LCPB mid-Ordovician into the Late Silurian. In the mid-Ordovician, L-chondritic micrometeorites make up >99% of the total flux. In the late Silurian, L chondrites make up about 60% of the ordinary chondritic micrometeorites, which is consistent with a remaining factor of two enhancement in the flux of such micrometeorites compared to background flux. The detailed results for the two sections studied here are discussed below.

Cellon Section

In the 321 kg of Silurian rock, 183 and 15 chrome-rich spinels were found in the 32–63 μm and the 63–355 μm fractions, respectively (Table 1; Table S1). Of these, 155 are EC (10 >63 μm), 12 Outlier EC, 16 OC-V, and 15 OC. Based on the TiO_2 content the 155 EC grains could be divided into H, L, and LL fractions of 33%, 56%, and 11%, respectively (Table 2). The three individual approximately 100 kg sized samples each contain circa 50 EC grains in the 32–63 μm fraction. The two lower samples show similar proportions between H, L, and LL grains, whereas the uppermost sample has a somewhat higher L/H ratio than the samples below. The average amount of EC grains in the >63 μm fraction is 3 grains per 100 kg for comparison with the Ordovician sample. Using a density of 2.58 g cm^{-3} for the limestone (measured using Archimedes principle on a small piece of sample S-30) and a sedimentation rate of 4 mm per ka gives an EC accumulation rate of 0.32 grain >63 μm m^{-2} ka^{-1} (Fig. 3). The EC grains often are very angular to subangular in shape, most have irregular fractures to some extent, and a few have reaction rims.

The Outlier EC grains consist of seven MgO-enriched and five MgO-depleted. The MgO-enriched grains have 6.20–8.56 wt% MgO content, and three of the grains have MnO+FeO+ZnO <23 wt%. The MgO-depleted grains have MgO contents ranging from 0.22 to 0.85 wt%, and ZnO from 1.23 to 14.9 wt% (see Table S1). The polished MgO-depleted grains are heavily fractured, but show no obvious signs of zoning or reaction rims. The MgO-enriched grains typically have fractures, and half of the grains also have bands of small spots of a darker mineral phase, in the vicinity of fractures and in the rim.

Of the 16 OC-V grains, 9 are found in the lowermost sample and 4 and 3 in the two upper samples, respectively. The ratio of EC/OC-V grains is on average 10, but this varies significantly between the three samples. The lowermost sample has a ratio of 6, compared to 13 and 17 in the overlying beds. A TiO_2 content higher than 4.0 wt% was detected in two grains from sample S-24, with 4.84 and 9.24 wt%, respectively. The latter grain is small (~40 μm), has an irregular surface due to many parallel and subparallel joints and dislocations, and low total oxide weight percentage (~86 wt%).

Of the 15 Silurian OC grains, almost all of the OC grains are likely terrestrial. When plotting the grains in the major element compositional fields of terrestrial Cr-spinels, the grains have the best fit with ophiolites, however, in mainly Cr# versus Fe# (Fig. 4). Mostly grains from the two uppermost samples fall outside of the density plot fields. Compared to both the EC and the OC-V grains, the OC grains have very different ratios between grains in the small and the large size fractions. The EC and OC-V grains have a ratio around 15, whereas the OC grains lie at three.

Killeröd Section

The Ordovician sample of 102 kg rock contains 498 (>63 μm) Cr-spinel grains in total (Table 1; Table S1). Of these 444 are EC, 30 Outlier EC, 8 OC-V, and 16 OC grains. The fractions of H, L, and LL of the 444 EC grains are 14%, 81%, and 5%, respectively (Table 3). The amount of EC grains in the large fraction is 4.3 grains kg^{-1} (4.6 grains kg^{-1} including the Outlier EC grains). Using the density 2.54 g cm^{-3} (as calculated from a small rock sample) and sedimentation rates in the range 2–4 mm per ka gives an EC accumulation rate in the range of 22–44 grains >63 μm m^{-2} ka^{-1} (Fig. 3). The EC grains are generally angular/very angular in shape (75%) and based on 100 randomly selected images of polished EC grains, around 80% have fractures and ~45% have reaction phases in rims and fractures.

Twenty-three of the EC Outlier grains have no MgO content and/or below the detection limit and two grains have 0.53 and 0.74 wt% MgO, respectively. The

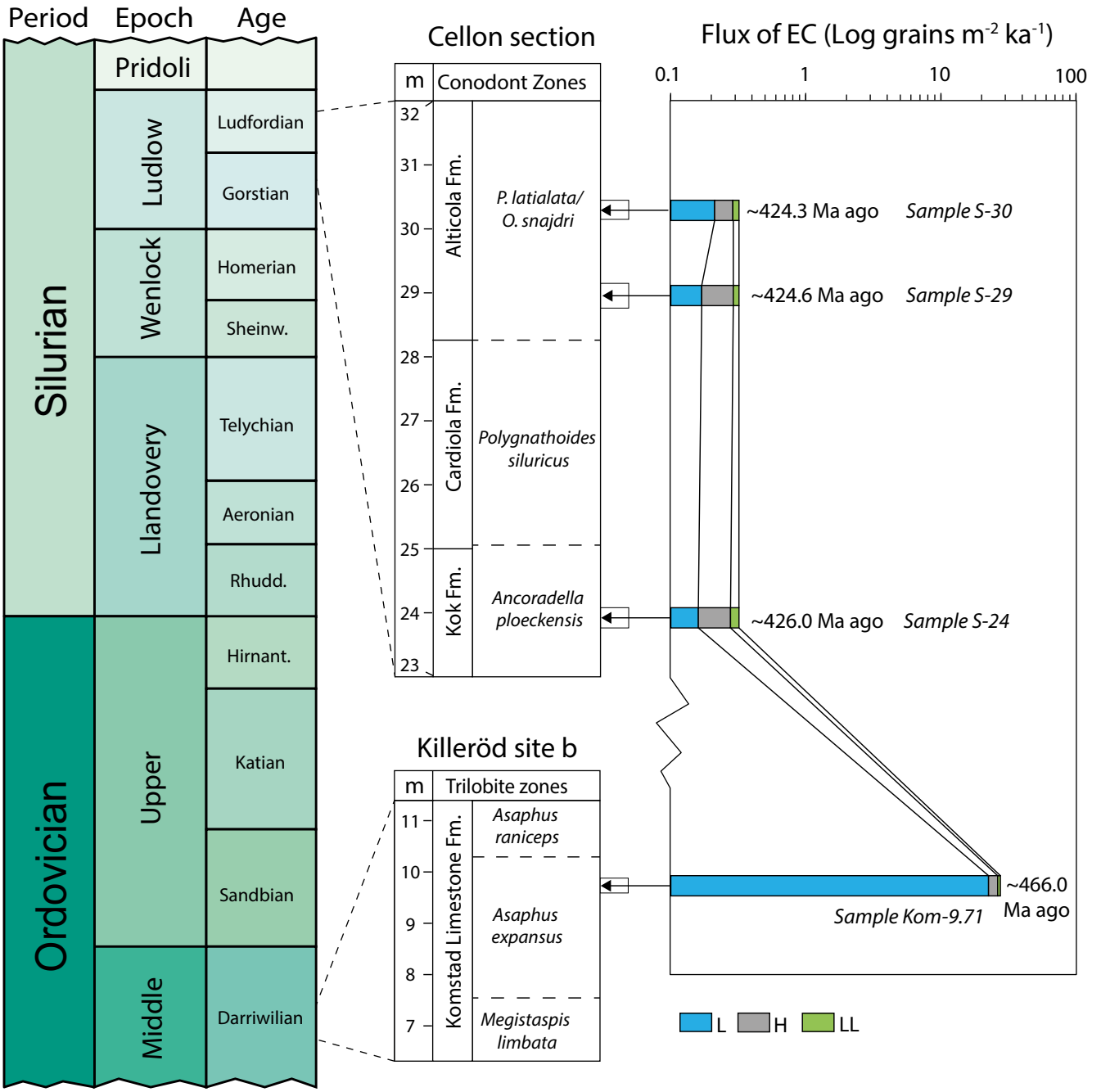

Fig. 3. Sample location in the stratigraphic column with the flux of EC grains m^{-2} ka^{-1} estimated in this study. The mid-Ordovician column is based on an estimated average sedimentation rate of 2.5 mm ka^{-1}, approximated from the sedimentation rate of the Hällekis and Thorsberg quarries and the difference in thickness of the *Asaphus expansus* trilobite zone at the Komstad Limestone Formation at Killeröd and the two former quarries.

ZnO content of the grains varies between 2.85 and 9.86 wt%. The seven MgO-enriched grains have MgO contents of 6.34–9.49 wt%. Almost 90% of the grains are fractured. More than half (13 of 25) of the polished MgO-depleted grains have surfaces covered by small dark spots (<1 μm) (Fig. 5).

The eight OC-V grains have high Cr# and Fe# and low Fe/3+#, and TiO_2 of 0.46–2.48 wt%. Grains 361, 405, and 409 have totals between 91.2 and 94.0 wt%, which could indicate that the data are somewhat unreliable. All grains have irregular fractures to some extent. All of these grains plot outside of terrestrial

Table 1. Summary of chrome-spinel grains found in this study.

Sample	Sample weight (kg)	EC > 63 μm	Outlier EC >63	OC-V > 63 μm	OC >63 μm	EC 32–63 μm	Outlier EC 32–63 μm	OC-V 32–63 μm	OC 32–63 μm	Grain total
S-30	103	2	–	0	0	48	4	3	2	59
S-29	108	3	–	1	2	50	4	3	6	69
S-24	109	5	–	0	2	47	4	9	3	70
Total	321	10	–	1	4	145	12	15	11	198
Kom-9.71	102	444	30	8	16	–	–	–	–	498

Table 2. Division of Late Silurian equilibrated ordinary chondritic (EC) grains using TiO_2 (wt%).

TiO_2 (wt%):	H ≥2.51%	L 2.51–3.39%	LL ≥3.40%
S-30 [n = 50)	12	33	5
%	24	66	10
S-29 [n = 53]	20	28	5
%	38	53	9
S-24 [n = 52]	19	26	7
%	37	50	13
Total Late Silurian [n = 155]	51	87	17
%	33	56	11

compositional fields. A majority of the grains have compositions similar or identical to EC grains, but with very low TiO_2, which could indicate that they are from unequilibrated ordinary chondrites. The ratio of EC/OC-V grains in the Komstad Limestone is 56.

In the data density plots by Barnes and Roeder (2001) with compositional fields of terrestrial Cr-spinel of differing magmatic regimes (Fig. 4), the OC grains have the best fit with ophiolitic Cr-spinels; however, in Cr# versus Fe# the majority of the grains plot within the 90th percentile area of the compositional field, but outside of the densest 50th percentile area. Four grains also plot outside of the ophiolitic field in the plot of TiO_2 and Fe/3+# as these grains have relatively high TiO_2 and very low Fe/3+#. For these two ratios, these four grains do not plot inside any of the compositional fields presented in Barnes and Roeder (2001).

We found six Cr-spinel grains containing nickel, one of which is categorized as Outlier EC, and two as EC grains (the other three grains as OC). EC grain #243 has a typical EC chemistry and appearance and is angular to subangular with many irregular and subparallel fractures. The nickel content is highest toward the rim with no or very little content in the center. The other EC grain and the Outlier EC grain rich in NiO are also enriched in MgO. Unpolished, the two grains appear as pyramidal aggregates (Fig. 6). As polished grains the surfaces appear "spongy" and "melted." The content of NiO is 0.55 and 0.61 wt%, respectively, with a more or less homogeneous distribution throughout the grains. Three of the OC grains also contain nickel (0.75–0.84 wt% NiO). These grains have a melted appearance when polished. Two of the grains have a zoned structure, or "onion"-layered–like structure. The third grain (#48) is very small and has an uneven structure. One grain (#94) has a chemical composition with some resemblance to grains from the fossil meteorite Österplana 065, an "extinct" type of meteorite with a primitive achondritic oxygen isotopic composition (Schmitz et al. 2016). However, about six grains with similar compositions were found by Häggström and Schmitz (2007) in the layer just above the sampled one in this study. These grains were found together with 51 other OC grains. A high OC/EC ratio of the sample indicates that most OC grains, including the six grains with Österplana 065 similarities, most likely are terrestrial.

DISCUSSION

Ordovician-to-Silurian Change in Flux of Ordinary Chondrites

The results for the Cellon section show that 40 Ma after the LCPB the micrometeorite flux has almost returned to background levels (Fig. 3). Our results for the Komstad Limestone leave little doubt that there was a two orders of magnitude enhancement in the flux of L-chondritic meteorites to Earth during a few million years after the LCPB. The similar lithology and facies, condensed orthoceratite limestone, in the two sections studied here make any comparisons of the flux as robust as it can be. The comparison is straightforward, the Komstad Limestone contains 434 EC grains (>63 μm) (or 463 including EC Outlier grains) per 100 kg, and the Cellon Limestone 3 EC grains per 100 kg. Within a factor of two the sections formed at the same sedimentation rate. Including the new Late Silurian results, we now have statistically relevant micrometeorite data for large sediment samples from four different time periods outside the immediate post-LCPB interval (Table 4). The periods studied previously are the pre-LCPB mid-Ordovician, Early Cretaceous, and the latest Maastrichtian-earliest Paleocene (Cronholm and Schmitz 2007; Heck et al. 2017; Schmitz

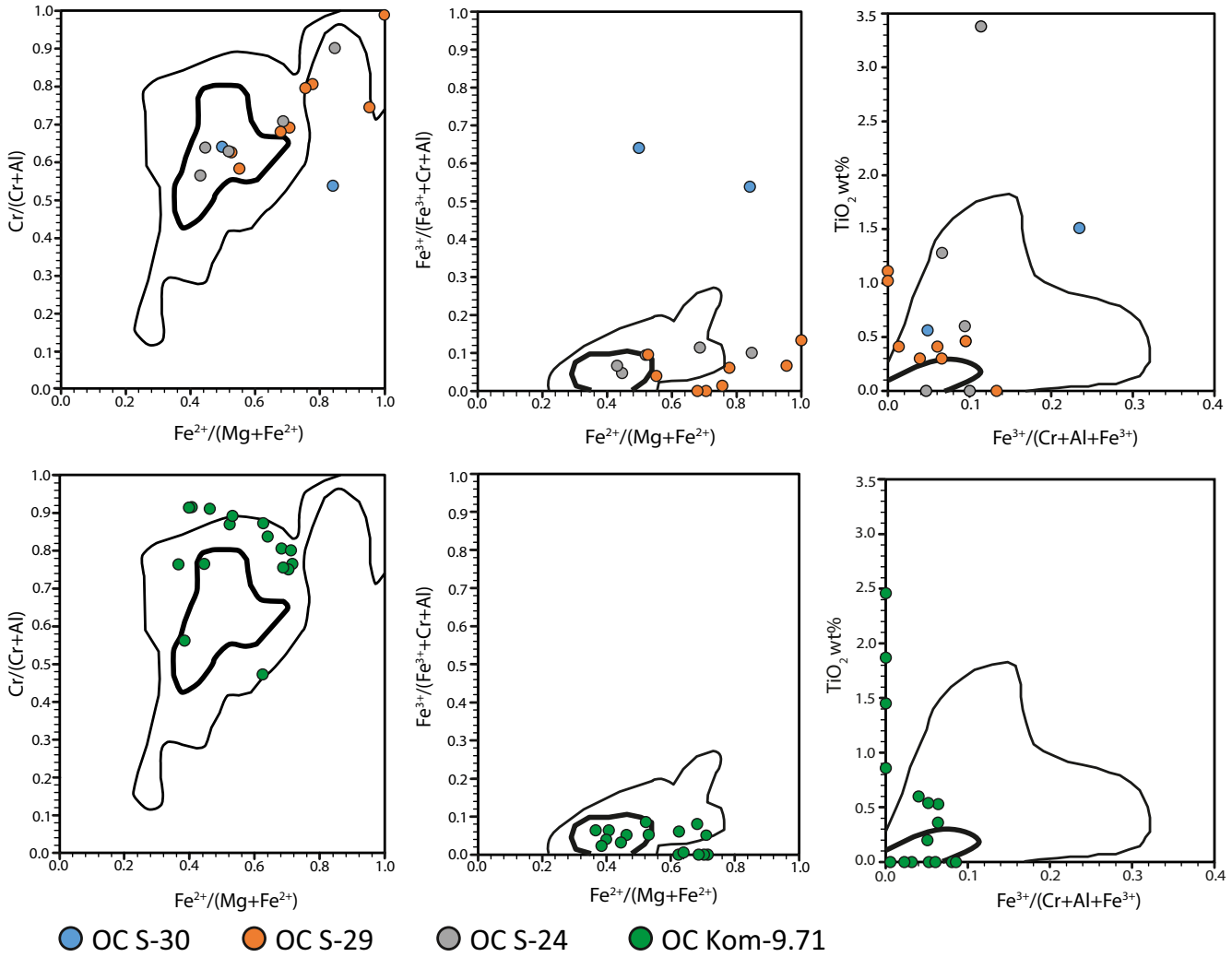

Fig. 4. Chemical composition of the OC grains from the Late Silurian and the mid-Ordovician samples plotted against the compositional density contour fields within which 90% (thin line) and 50% (bold line) of spinels from ophiolitic rocks according to Barnes and Roeder (2001). Complete grain data from EDS analysis available in Table S1.

et al. 2017). The micrometeorite flux appears very similar during the four periods, 0.1–0.3 grains m^{-2} ka^{-1}, which likely represents the typical background flux through the Phanerozoic.

We only have data in the >63 μm fraction for the Komstad Limestone sample because it would be a too tedious task to quantify the grains in the 32–63 μm fraction. In the Cellon section, we see that the ratio between the number of grains in the 32–63 μm fraction versus the >63 μm fraction is approximately 15. Assuming the same ratio for the Komstad Limestone would imply that our 102 kg of Komstad Limestone contains about 7000 EC grains in the smaller size fraction. This is in line with our pilot studies of the size fraction ratios in many pilot samples, 1–15 kg large, from different time periods where the ratios typically lie in the range 15–25.

The distribution of EC grains in the three different TiO_2 ranges corresponding to the H, L, and LL ordinary chondrites shows that in the Late Silurian there is still an overrepresentation of L-type meteorites in relation to H and LL, compared to the three other background time windows for which we have similar data (Tables 3 and 5). The division of the Silurian grains corrected for overlap in TiO_2 between chondrite groups indicate ~60% L chondrites (among ordinary chondrites) in the Late Silurian compared to ~100% in the immediate post-LCPB interval and ~35–45% during the three background time windows for which we have data (Fig. 7). The latter value is similar to the present-day percentage of ~45% L chondrites among the ordinary chondrites. The finding that in the Late Silurian the flux of the L chondrites was still higher

Table 3. Division of equilibrated ordinary chondritic (EC) grains using TiO_2 (wt%) for different time windows.

TiO_2 (wt%)	H ≥2.51%	L 2.51–3.39%	LL ≥3.40%
Early Cretaceous [n = 81][a] Monte Acuto and Bosso River sections	36	34	11
%	44	42	14
Late Silurian [n = 155][b] Cellon section	51	87	17
%	33	56	11
Mid-Ordovician post-LCPB [n = 444][b] Killeröd site b	63	361	20
%	14	81	5
Mid-Ordovician post-LCPB [n = 119][c] Hällekis quarry and Lynna River section	10	102	7
%	8	86	6
Mid-Ordovician pre-LCPB [n = 215][a,d] Lynna River section	80	71	64
%	37	33	30

[a]Schmitz et al. (2017); [b]This study; [c]Heck et al. (2016); [d]Heck et al. (2017).

compared to H and LL chondrites than during background conditions may appear contradictive to the finding that the flux had almost returned to background levels. However, this only reflects the crudeness of the flux estimates, i.e., we measure a decrease to a "normal" flux from a two orders of magnitude enhancement. The flux in the mid-Ordovician pre-LCPB and Early Cretaceous indicates that the background flux is closer to around 0.1 grains m^{-2} ka^{-1}. The enhanced L/H ratio in the Late Silurian compared to background can be explained by only a factor of two enhancement in the flux of L chondrites. It is noted that without detailed data in the 40 Ma between the two time windows it cannot be ruled out that the slight enhancement of L chondrites in the Late Silurian could be due to secondary collisions between remnant smaller L chondrite bodies in the asteroid belt. Even so, examining the shock-ages of L-chondritic meteorites there is a distinct sharp spike around 470 Ma ago. There is also a smaller, less distinct peak around 430 Ma ago; however, this peak appears because of the large uncertainties in the ages of some meteorites overlapping around this age (Swindle et al. 2014).

The three samples from the Cellon section span over two million years and provide some insights into the stability of the flux over such time frames. Each bed yields about 50 EC grains in the small fraction indicating relatively stable flux for ordinary chondrites over two million years (assuming stable sedimentation rates). The slightly different ratios of H, L, and LL grains in the uppermost sample compared to the two samples below may simply reflect a statistically insufficient number of grains for any more detailed conclusions. For a more robust case, data for >100 grains per bed would have been required. It must be emphasized that a random, single larger micrometeorite with several Cr-spinel grains included in one of our samples would bias the results. That is why we rely mainly on averages based on samples from different beds or sites.

The results for the Ordovician sample are consistent with previous work from Killeröd (Häggström and Schmitz 2007) where the studied interval yielded 4.5 EC grains kg^{-1} in the >63 μm. For comparison, coeval post-LCPB Orthoceratite Limestone yields in the same size fraction 5–10 EC grains kg^{-1} in the Lynna River section, Russia, and 1–3 EC grains kg^{-1} in the Hällekis quarry (Schmitz and Häggstrom 2006; Lindskog et al. 2012). The small differences in grain abundance reflect mainly variations in sedimentation rates at the different localities. The mid-Ordovician strata in the Killeröd section have been cut off by erosion and end a few meters above our studied sample. In the Hällekis quarry at Kinnekulle, however, which contains younger beds, a decline in EC grain abundance by a factor of 10 (0.4 EC grains kg^{-1}), could be seen in the youngest Ordovician sample studied at about 10 m above the Volkhov–Kunda boundary (~2 m below the base of the Arkeologen bed in the Hällekis quarry) that probably corresponds in time to the LCPB (Schmitz and Häggström 2006; Schmitz et al. 2008). From the cosmic ray exposure ages of fossil meteorites (Heck et al. 2008) the sedimentation rate in the Hällekis and Thorsberg quarries at Kinnekulle could be estimated to be around 3.4 mm per ka (~3 m between the middle of Arkeologen bed up to the middle of Goda Lagret, the time between the exposure ages of the meteorites in those layers is ~900 ka). This indicates that the flux from the LCPB had decreased by one order of magnitude about 2.5–3 Ma after the breakup. Further support of such a decline relates to the fossil Brunflo L chondrite in the Gärde quarry in Jämtland (the first ever fossil meteorite find; Thorslund et al. 1984). It resides in strata that formed 4–5 Ma after the LCPB. In this younger interval, sediment-dispersed EC grains were also found with an average EC content of 0.45 grains kg^{-1} (Alwmark and Schmitz 2009). This would imply a steady rate of micrometeorite flux over a couple of million years; however, as discussed by the previous authors, variations in sedimentation rate on small scales cannot be determined. In light of the combined results of the different studies the full decline in the flux by two

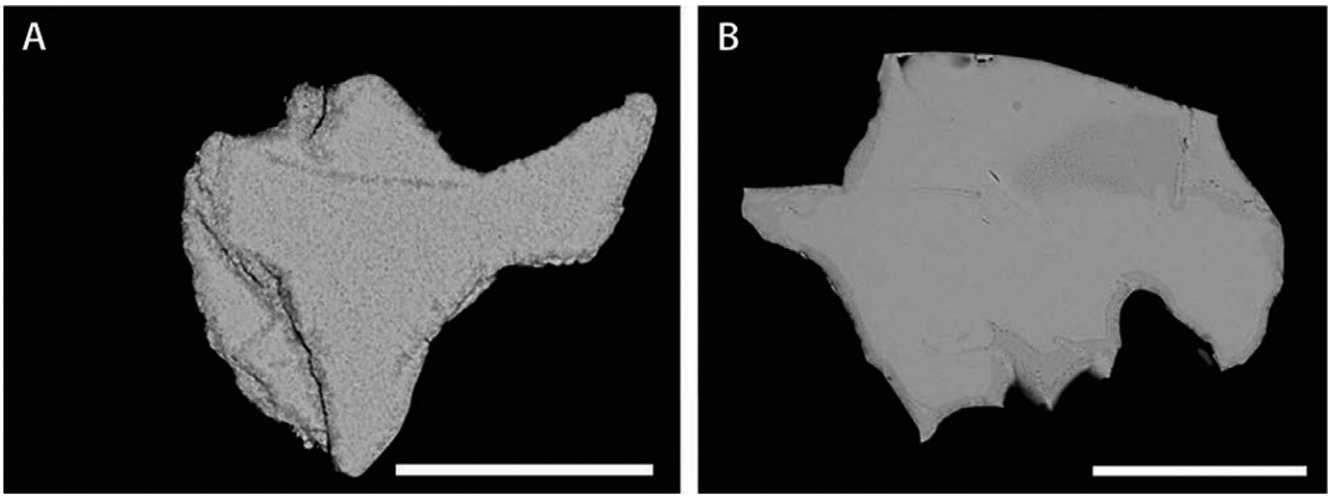

Fig. 5. Backscattered SEM images of A) MgO-depleted Outlier EC grain (#249) with the common spotty appearance and B) of EC grain #393 with reaction rims in which small inclusions of a darker phase is visible. Scale bar = 50 μm.

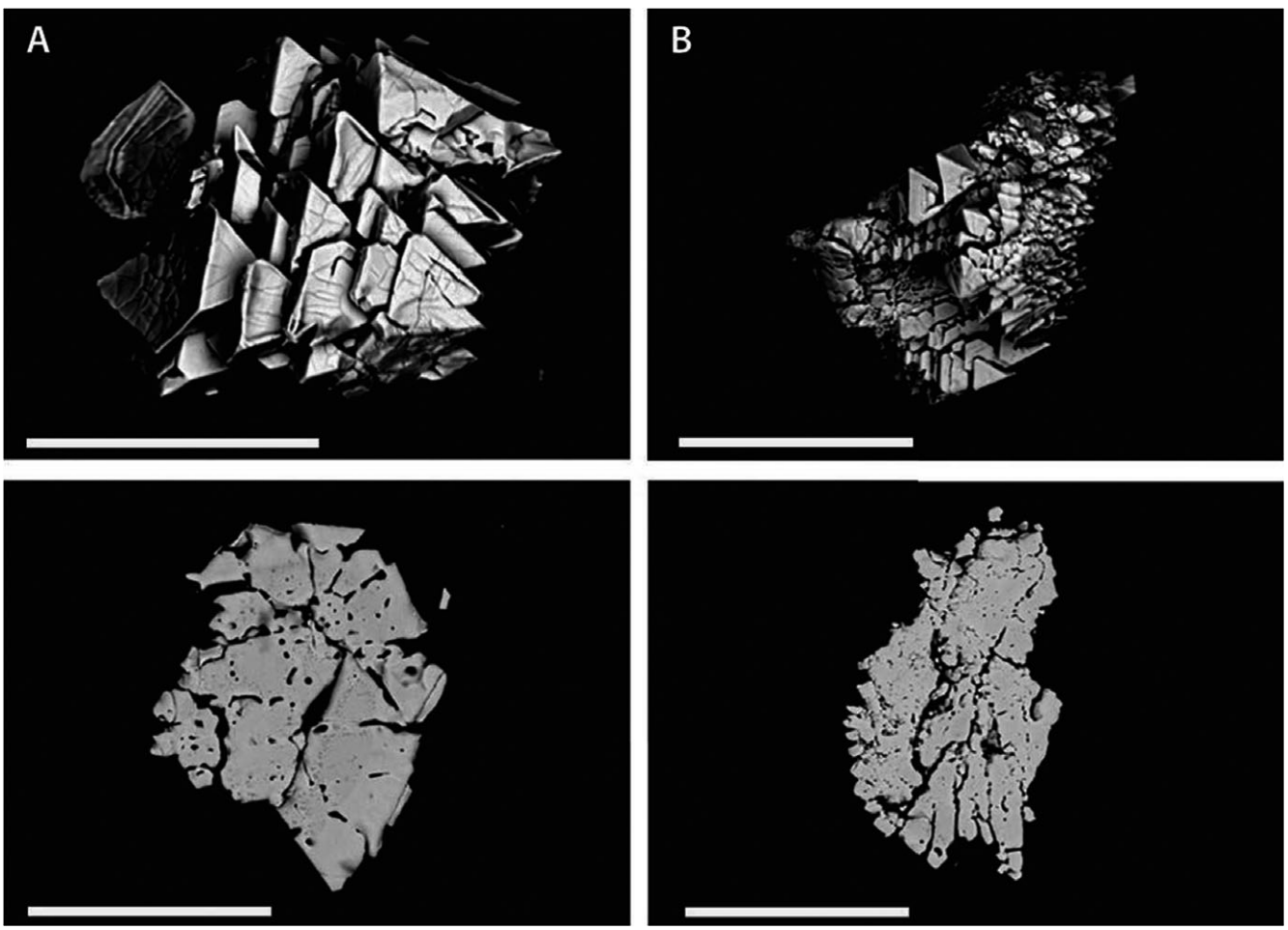

Fig. 6. Backscattered SEM images of unpolished and polished nickel-containing (A) Outlier EC grain #305 and (B) EC grain #497. Scale bar = 50 μm.

Table 4. Equilibrated ordinary chondritic (EC) grains >63 μm during different time windows.

Study	Weight (kg)	#EC grains >63 μm	Grains per 100 kg	Sedimentation rate (mm ka^{-1})	Flux (grains m^{-2} ka^{-1})
Early Danian[a]	140	5	3.6	2.5	0.23
Late Maastrichtian[a]	70	1	1.4	5.0	0.18
Early Cretaceous[b]	1652	2	0.1	25.0	0.075
Late Silurian[c]	321	10	3.1	4.0	0.32
Mid-Ordovician post-LCPB[c]	102	444	434	2.5	27
Mid-Ordovician pre-LCPB[d]	379	5	1.3	3.5	0.11

[a]Cronholm and Schmitz (2007); [b]Schmitz et al. (2017); [c]This study; [d]Schmitz and Häggström (2006).

Table 5. Division of equilibrated ordinary chondritic (EC) grains using TiO_2 (wt%) and correction of the 10% overlap between the three groups.

TiO_2 (wt%):	H ≤2.50%	L 2.51–3.39%	LL ≥3.40%
Early Cretaceous [n = 81][a]	36.2	36.1	7.7
%	45	45	10
Late Silurian [n = 155][b]	47.4	97.6	10
%	31	63	6
Mid-Ordovician post-LCPB [n = 444][b]	33.2	424.9	−14.1
%	7	96	−3
Mid-Ordovician post-LCPB [n = 119][c]	0.8	120.7	−2.5
%	1	101	−2
Mid-Ordovician pre-LCPB [n = 215][a,d]	80.9	71.2	63.3
%	38	33	29

[a]Schmitz et al. 2017; [b]This study; [c]Heck et al. 2016; [d]Heck et al. 2017.

Table 5 shows the percentages of H, L, and LL EC grains with the 10% overlap between the three groups. The overlaps are calculated and subtracted or added to respective group. When a group has a large percentage, as in e.g., Post-LCPB L group grains, then this can cause a false negative grain count and group percentage in the groups with low percentage.

orders of magnitude occurred somewhere between 4 and 40 Ma after the event. Extrapolating from the decrease of one order of magnitude at ~3 Ma after the LCPB implies that the flux would have decreased to around background levels already at ~6 Ma after the breakup event.

OC-V Grains

In the Silurian beds in the present study, 16 OC-V grains were found. Most or all of these grains are likely of extraterrestrial origin, based on (1) a high OC-V/OC ratio in the beds (i.e., few terrestrial spinel grains in the sample), (2) a "reasonable" EC/OC-V ratio of 10, and (3) similar size fraction ratios for OC-V grains as for EC grains, but different from OC grains (see Results section). In order to understand the detailed origin of OC-V grains, oxygen isotope data are required. For two of the time windows for which previously detailed micrometeorite flux reconstructions have been made, most of the OC-V grains were analyzed for both elemental and oxygen isotopic composition (Heck et al. 2017; Schmitz et al. 2017). In a sample from the mid-Ordovician just before the LCPB, the OC-V/EC grain ratios are exceptionally low, 1.5, and in the Early Cretaceous time window, the ratio was found to be 3 (Table 6). In both studies, the oxygen isotopes confirmed that all or the clear majority of the OC-V grains are extraterrestrial. Most of the grains are from different types of achondrites, with another significant fraction originating from unequilibrated ordinary chondrites. The high EC/OC-V ratio of 10 in the Silurian time window is similar to the ratio between ordinary chondrites and achondrites in the meteorite flux today. However, to compare Cr-spinel grain ratios to actual meteorite ratios is not a straightforward process. In the study by Heck et al. (2017), 13 achondritic meteorites were dissolved and their content of chrome-spinel (>63 μm) were seen to be less per mass than in ordinary chondrites. In any case, the high EC/OC-V ratio of the Silurian sample speaks against the idea forwarded by Schmitz et al. (2017) based on two flux windows and the modeling arguments in Heck et al. (2017) that there was a gradual decline in the ratio between the flux of primitive achondrites and ordinary chondrites through the Phanerozoic. The results in the present study indicate a more complex scenario with shorter turnovers in meteorite assemblages reaching Earth than envisioned by Heck et al. (2017) and Schmitz et al. (2017). Clearly, data from more windows are required in order to create a robust understanding of how the micrometeorite flux to Earth is changing over deep time.

The lowest Silurian sample contains nine OC-V grains compared to ~3 grains each in the two upper samples. The significantly higher content of OC-V grains in the lowermost sample compared to the

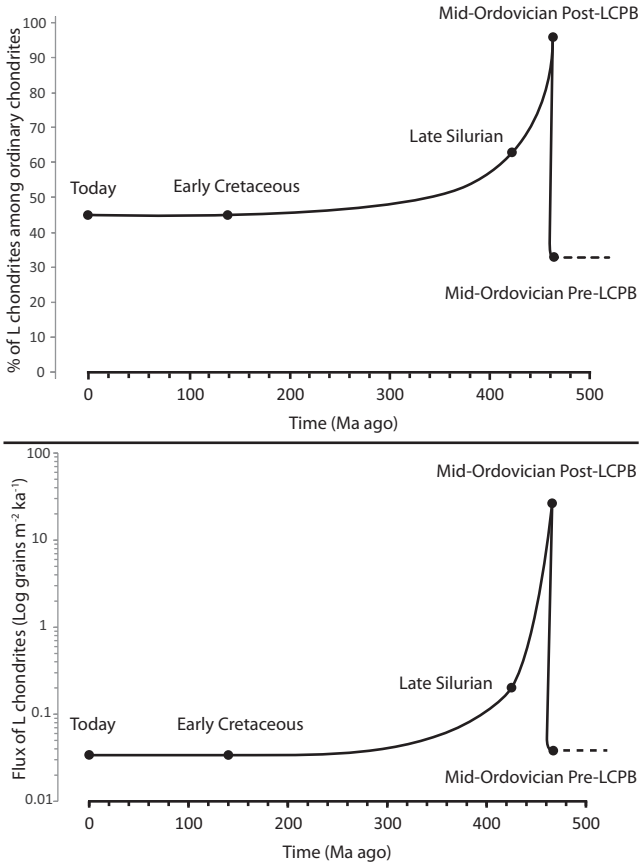

Fig. 7. A) Graph showing the rise and decay of the percentage of L chondrites during the four time windows and today in which there is sufficient data. B) Graph showing the flux of L chondrites through the four time windows until today. The fraction of L chondrites is based on both the small (32–63 μm) and the large (>63 μm) fraction of EC grains but the total flux is calculated from the large fraction only. The recent flux is assumed to be at/within background values and is set to that of the Early Cretaceous (see Schmitz et al. 2017).

superjacent samples is an enigma. Based on elemental content the grains in the lower sample may originate from a few different types of unusual micrometeorites, but without oxygen isotopic results this cannot be elaborated further. If grouping these grains by chemical composition then they represent 3–4 types of grains. As shown in Heck et al. (2017), achondritic chrome-spinels sometimes belong to the same meteorite group and have similar composition, but the chemistry can also vary for grains with similar origin. Some of the Silurian OC-V grains could be from unequilibrated ordinary chondrites as the composition overall is similar or identical to equilibrated ordinary chondritic grains, except for a much lower TiO_2 value. Two OC-V grains have TiO_2 content >4 wt% of which one grain from sample S-24 has almost 10 wt% TiO_2. Chrome-spinels with high titanium (>4 wt%) and vanadium content (>0.5 wt%) are less common on Earth than in lunar spinels (Papike et al. 1991). The relatively low EC/OC-V ratio of 4.7 of the lowermost Silurian sample could better reflect the "true" achondrite flux to Earth than the two upper samples (poor statistics) but could also be the result of just a few larger micrometeorites from the same source that settled in the sediments of the lowest sample. The high number of OC-V grains in the lowest Silurian sample, which is the most anoxic (high organic content), cannot be readily explained by differences in diagenetic environment considering that all the samples contain equal amounts of diagenetically altered Outlier EC grains (see below). The OC-V grains are interesting for further isotopic analysis as they might contain grains from rarer meteorite types as demonstrated by Schmitz et al. (2017). In their study of Early Cretaceous sediments, where 17 OC-V grains were analyzed for O-isotopic composition, 12 of the grains belonged to achondritic meteorites and 5 likely belonged to unequilibrated ordinary chondrites.

The EC/OC-V ratio in the post-LCPB mid-Ordovician Komstad sample is very high, 56, reflecting the total dominance of L-chondritic micrometeorites. No Cr-spinel grain was found that could unambiguously be related to lunar debris (from secondary collisions) or to the type of "extinct" primitive achondrite represented by the Österplana 065 fossil meteorite. The OC/OC-V ratio in the Komstad sample is low, 2, indicating that most of the eight OC-V grains found are extraterrestrial, most likely from unequilibrated L chondrites.

OC Grains

The vast majority of the OC grains are probably of terrestrial origin. The OC grains from both the Cellon and the Killeröd section fit best with ophiolitic spinels, but some grains deviate, which could be due to diagenetical alteration, as seen in the Outlier EC grains. Some of the OC grains can be from rare types of meteorites/achondrites with Cr-spinels low in V_2O_3. Three Cr-spinel grains found in pre-LCPB strata in Russian sediments (Heck et al. 2017) had V_2O_3 contents between 0.3 and 0.44 wt%, but an oxygen isotopic composition consistent with a meteoritic origin. The other OC grains that possibly are extraterrestrial in the present study are those in the Komstad Limestone that contain NiO. Grains with similar compositions and appearances were found in Russian coeval sediments (Lindskog et al. 2012), with enrichment of MgO and deficit in FeO, and in aggregate EC grains from the mid-Ordovician Lockne crater resurge deposits (Alwmark and Schmitz 2007). The aggregate EC grains also have a melted and spongy appearance when

Table 6. Comparison of fluxes of different meteorite types in different time periods. Modified from Schmitz et al. (2017).

Type of chrome-spinel[d]	Pre-LCPB Ordovician[a] # (%) of grains	Post-LCPB Ordovician[b] # (%) of grains	Late Silurian[c] # (%) of grains	Early Cretaceous[c] # (%) of grains	Today[e] % of flux
EC	23 (56)	444 (98)	155 (91)	81 (75)	90
OC-V	15 (37)	8 (2)	16 (9)	27 (25)	9
AC-low-V	3 (7)	N/A	N/A	N/A	<1
EC/OC-V ratio[f]	1.5	56	10	3	10

[a]Heck et al. (2017); [b]This study; [c]Schmitz et al. (2017).

[d]EC = chromite from equilibrated ordinary chondrite; OC-V = other chrome-spinel with V_2O_3 ≥0.45 wt%; AC-low-V = chrome-spinel from achondrites judging from $\Delta^{17}O$ value below terrestrial fractionation line, but with V_2O_3 ≤0.44 wt%.

[e]Fraction of the flux excluding the recent major meteorite groups poor in large Cr-spinel. The OC-V category as defined for this column includes all achondrites rich in Cr-spinel with high (>0.5 wt%) V_2O_3, as well as the R chondrites and unequilibrated ordinary chondrites. The AC-low-V category includes achondrites rich in Cr-spinel but with low (<0.45 wt%) V_2O_3. Source: Meteoritical Bulletin database (www.lpi.usra.edu/meteor/).

[f]The ratios for the Ordovician, the Silurian, and the Cretaceous are not directly comparable to the ratio for today's flux. Most achondrites and unequilibrated ordinary chondrites have significantly lower contents of chrome-spinels (>32 μm) than the equilibrated ordinary chondrites. If this could be accounted for, the Ordovician, Silurian, and Cretaceous ratios would be even lower than given here. Ideally, comparisons between different time periods should be based entirely on variations in the types of chrome-spinel grains recovered from sediments.

N/A = not applicable.

polished just as the grains containing NiO in this study. When meteorites enter the Earth's atmosphere, the outermost crust of the meteorite is heated by friction that causes melting and the crust becomes ferromagnetic because of magnetite formation in the crust (Ramdohr 1967; Genge and Grady 1999; Parashar et al. 2010). Chondrite fusion crusts contain Ni-rich sulfide droplets that when in a melted state could diffuse Ni into adjacent unmelted chromite grains that resided in close vicinity to the crust. The ratio between the small and large fractions in the Cellon samples is much lower for the OC grains than for the EC and OC-V. This indicates that the OC grains reached the sea floor through another transport mechanism than the EC and OC-V grains, probably involving hydrodynamic sorting (e.g., coarser mineral grains accumulating near shore, that later can be redistributed by strong currents to the deep sea).

Outlier EC Grains

Both in the Ordovician and Silurian beds in the present study, the Outlier EC grains represent about 7% of the total amount of EC grains. This is higher than in the mid-Ordovician limestone at Kinnekulle in Sweden and the Lynna river section in Russia. At Lynna, Lindskog et al. (2012) found 307 EC grains (data from unpolished grains are excluded) of which seven are Outlier EC grains corresponding to approximately 2% of the total number of EC grains. Only one of the Outlier EC grains is MgO-depleted, the rest are MgO-enriched. Out of 335 EC grains found by Schmitz and Häggstrom (2006) in Kinnekulle limestone, only one grain was an Outlier EC grain (MgO-enriched). A possible explanation to the higher content of Outlier EC grains in the limestones of the present study is that they were formed in more stagnant environments leading to reducing conditions than the mainly oxidized limestones of previous studies. Reducing suboxic to anoxic conditions may be more diagenetically aggressive on the Cr-oxides. This may explain specifically the occurrence of MgO-depleted grains that have not been found in similar quantities in any of the other studied sections. All samples from both sections studied here have relatively large amounts of metal sulfides in the undissolved residue. These can form during shallow burial at low temperatures where sulfate is reduced in the presence of organic matter in which the organic compounds oxidize. Through this reduction of sulfate, hydrogen sulfide is formed that further reacts with iron minerals to form metal sulfides (Berner 1984; Machel 2001). The surfaces of polished MgO-depleted grains from Killeröd are covered by small spots <1 μm distributed evenly from core to rim, but usually concentrates around fractures. This pervasive appearance is not seen in EC, OC-V, or OC grains. Except for being heavily fractured, the Silurian outlier grains do not show signs of chemical alteration; however, the grains are much fewer than in Killeröd. The grains may be highly vesicular/porous possibly related to partial melting during passage through the atmosphere. Previous studies also confirm that MgO and FeO are the oxides most commonly affected by diagenesis and TiO_2 the most stable. Many EC grains also have reaction rims that likely formed after deposition in contact with the sediment and pore-water. The exclusion of the Outlier EC grains only makes a small difference in the H, L, and LL ratios, but should

nonetheless be excluded to make the grain definitions valid. Almost 40% of the 30 Outlier EC grains have TiO_2 content as that of H-chondritic grains. This could just be a statistical bias, or that H-chondritic grains are more susceptible to alteration, alternatively that the otherwise stable TiO_2 content has been affected by diagenesis in these grains. In Heck et al. (2016) a slightly larger part of the EC grains found were L chondritic (Table 5). This could possibly be due to the reducing depositional environment in Killeröd being harsher on the grains.

SUMMARY AND CONCLUSIONS

Our data show that in the Late Silurian the flux of ordinary equilibrated (L) chondrites had dropped by two orders of magnitude following the large increase in L-chondritic meteorites to Earth during the mid-Ordovician. The L chondrites still slightly dominated over both H and LL chondrites. This indicates that the flux of L chondrites was still slightly enhanced ~40 Ma after the LCPB that may have been caused by secondary disruptions of smaller remnant L-chondrite asteroids.

The sediments in both the Silurian and mid-Ordovician section studied here formed in a reducing environment giving rise to alteration of a small percentage of the EC grains, and possibly also some of the OC and OC-V grains. This finding is important for the interpretations of past fluxes and what types of grains are found.

The flux of potential achondritic micrometeorites in the Late Silurian was similar to the present flux. The higher ratio between EC and OC-V grains compared to the time windows pre-LCPB and Early Cretaceous also indicates that there is a decrease in the number of achondrites in the Silurian that then increases again in the Early Cretaceous. Our data support the "waning-off" model, where one type of asteroid family is formed through a disruption event, leading to a sudden increase in the flux of one type of meteorite that slowly fades away in the rock record. The data, however, also indicate that this model must be complemented with other processes in order to explain the meteorite flux to Earth in deep time. A more complete record of the past meteorite flux is important for the understanding and interpretations of the dynamics of the asteroid belt and the solar system as a whole.

As to the hypothesis of lunar meteorites being ejected from the lunar surface during an increased bombardment of the Earth–Moon system following the LCPB event, no high titanium OC-V grains were found in the mid-Ordovician sample, which is a bit surprising. Two Silurian OC-V grains have high TiO_2 (>4.0 wt%) which could potentially reflect a lunar origin.

The OC grains have chemical characteristics that fit reasonably with an ophiolitic source, but a few of the OC grains could also be of extraterrestrial origin.

Acknowledgments—This study was supported by an ERC Advanced Grant (ASTROGEOBIOSPHERE) to B. S. We thank A. Cronholm, F. Iqbal, and F. Terfelt for support in the field and the laboratory. We also thank two anonymous reviewers for helpful comments.

Editorial Handling—Dr. Christian Koeberl

REFERENCES

Alwmark C. and Schmitz B. 2007. Extraterrestrial chromite in the resurge deposits of the early Late Ordovician Lockne crater, central Sweden. *Earth and Planetary Science Letters* 253:291–303.

Alwmark C. and Schmitz B. 2009. The origin of the Brunflo fossil meteorite and extraterrestrial chromite in Mid-Ordovician limestone from the Gärde Quarry (Jämtland, central Sweden). *Meteoritics & Planetary Science* 44:95–106.

Artemieva N. A. and Shuvalov V. V. 2008. Numerical simulation of high-velocity impact ejecta following falls of comets and asteroids onto the Moon. *Solar System Research* 42:329–334.

Barnes S. J. and Roeder P. L. 2001. The range of spinel compositions in terrestrial mafic and ultramafic rocks. *Journal of Petrology* 42:2279–2302.

Berner R. A. 1984. Sedimentary pyrite formation: An update. *Geochimica et Cosmochimica Acta* 48:605–615.

Boschi S., Schmitz B., Heck P. R., Cronholm A., Defouilloy C., Kita N. T., Monechi S., Montanari A., Rout S. S., and Terfelt F. 2017. Late Eocene ^{3}He and Ir anomalies associated with ordinary chondritic spinels. *Geochimica et Cosmochimica Acta* 204:205–218.

Bottke W. F. Jr., Durda D. D., Nesvorný D., Jedicke R., Morbidelli A., Vokrouhlický D., and Levison H. F. 2005. Linking the collisional history of the main asteroid belt to its dynamical excitation and depletion. *Icarus* 179:63–94.

Brett C. E., Ferretti A., Histon K., and Schönlaub H. P. 2009. Silurian sequence stratigraphy of the Carnic Alps, Austria. *Palaeogeography Palaeoclimatology Palaeoecology* 279:1–28.

Bridges J. C., Schmitz B., Hutchison R., Greenwood R. C., Tassinari M., and Franchi I. A. 2007. Petrographic classification of Middle Ordovician fossil meteorites from Sweden. *Meteoritics & Planetary Science* 42:1781–1789.

Chen J. and Lindström M. 1991. Cephalopod Septal Strength Indices (SSI) and depositional depth of the Swedish Orthoceratite limestone. *Geologica et Palaeontologica* 25:5–18.

Cocks L. R. M. and Torsvik T. H. 2005. Baltica from the late Precambrian to mid-Palaeozoic times: The gain and loss of a terrane's identity. *Earth-Science Reviews* 72:39–66.

Cohen K. M., Finney S. C., Gibbard P. L., and Fan J. X. 2013. The ICS international chronostratigraphic chart. *Episodes* 36:199–204.

Corradini C., Corriga M. G., Mannik P., and Schönlaub H. P. 2014. Revised conodont stratigraphy of the Cellon section (Silurian, Carnic Alps). *Lethaia* 48:56–71.

Cronholm A. and Schmitz B. 2007. Extraterrestrial chromite in latest Maastrichtian and Paleocene pelagic limestone at

Gubbio, Italy: The flux of unmelted ordinary chondrites. *Meteoritics & Planetary Science* 42:2099–2109.
Cronholm A. and Schmitz B. 2010. Extraterrestrial chromite distribution across the mid-Ordovician Puxi River section, central China: Evidence for a global major spike in flux of L-chondritic matter. *Icarus* 208:36–48.
Farley K. A., Vokrouhlický D., Bottke W. F., and Nesvorný D. 2006. A late Miocene dust shower from the break-up of an asteroid in the main belt. *Nature* 439:295–297.
Genge M. J. and Grady M. 1999. The fusion crusts of stony meteorites: Implications for the atmospheric reprocessing of extraterrestrial materials. *Meteoritics & Planetary Science* 34:341–356.
Geyer G. 1894. Zur Stratigraphie der palaeozoischen Schichtserie in den Karnischen Alpen. *Verhandlungen der kaiserlich koniglichen Geologischen Reichsanstalt* 1894:102–119.
Haack H., Farinella P., Scott E. R. D., and Keil K. 1996. Meteoritic, asteroidal, and theoretical constraints on the 500 Ma disruption of the L chondrite parent body. *Icarus* 119:182–191.
Häggström T. and Schmitz B. 2007. Distribution of extraterrestrial chromite in Middle Ordovician Komstad Limestone in the Killeröd quarry, Scania, Sweden. *Bulletin of the Geological Society of Denmark* 55:37–58.
Heck P. R., Schmitz B., Bauer H., and Wieler R. 2008. Noble gases in fossil micrometeorites and meteorites from 470 Myr old sediments from southern Sweden, and new evidence for the L-chondrite parent body breakup event. *Meteoritics & Planetary Science* 43:517–528.
Heck P. R., Schmitz B., Rout S. S., Tenner T., Villalon K., Cronholm A., Terfelt F., and Kita N. T. 2016. A search for H-chondritic chromite grains in sediments that formed immediately after the breakup of the L-chondrite parent body 470 Ma ago. *Geochimica et Cosmochimica Acta* 177:120–129.
Heck P. R., Schmitz B., Bottke W. F., Rout S. S., Kita N. T., Cronholm A., Defouilloy C., Dronov A., and Terfelt F. 2017. Rare meteorites common in the Ordovician period. *Nature Astronomy* 1:1–6.
Histon K. 2012. The Silurian nautiloid-bearing strata of the Cellon Section (Carnic Alps, Austria): Color variation related to events. *Palaeogeography, Palaeoclimatology, Palaeoecology* 367–368:231–255.
Histon K. and Schönlaub H. P. 1999. Taphonomy, palaeoecology and bathymetric implications of the nautiloid fauna from the Silurian of the Cellon section (Carnic Alps, Austria). *Abhandlungen der Geologischen Bundesanstalt* 54:259–274.
Jaanusson V. 1973. Aspects of carbonate sedimentation in the Ordovician of Baltoscandia. *Lethaia* 6:11–34.
Kirchoff M. R., Chapman C. R., Marchi S., Curtis K. M., Enke B., and Bottke W. F. 2013. Ages of large lunar impact craters and implications for bombardment during the Moon's middle age. *Icarus* 225:325–341.
Koeberl C. 2002. Mineralogical and geochemical aspects of impact craters. *Mineralogical Magazine* 66:745–768.
Lindskog A. 2014. Palaeoenvironmental significance of cool-water microbialites in the Darriwilian (Middle Ordovician) of Sweden. *Lethaia* 47:187–204.
Lindskog A., Schmitz B., Cronholm A., and Dronov A. 2012. A Russian record of a Middle Ordovician meteorite shower: Extraterrestrial chromite at Lynna River, St. Petersburg region. *Meteoritics & Planetary Science* 47:1274–1290.
Lindström M. 1963. Sedimentary folds and the development of limestone in an early Ordovician sea. *Sedimentology* 2:243–292.
Machel H. G. 2001. Bacterial and thermochemical sulfate reduction in diagenetic settings—Old and new insights. *Sedimentary Geology* 140:143–175.
McEwen A. S., Moore J. M., and Shoemaker E. M. 1997. The Phanerozoic impact cratering rate: Evidence from the farside of the Moon. *Journal of Geophysical Research* 102:9231–9242.
Meier M. M. M., Schmitz B., Bauer H., and Wieler R. 2010. Noble gases in individual L chondritic micrometeorites preserved in an Ordovician limestone. *Earth and Planetary Science Letters* 290:54–63.
Meier M. M. M., Schmitz B., Alwmark C., Trappitsch R., Maden C., and Wieler R. 2014. He and Ne in individual chromite grains from the regolith breccia Ghubara (L5): Exploring the history of the L chondrite parent body regolith. *Meteoritics & Planetary Science* 49:576–594.
Nesvorný D., Vokrouhlický D., Morbidelli A., and Bottke W. F. 2009. Asteroidal source of L chondrite meteorites. *Icarus* 200:698–701.
Nielsen A. T. 1995. Trilobite systematics, biostratigraphy and palaeoecology of the Lower Ordovician Komstad Limestone and Huk Formations, southern Scandinavia. *Fossils and Strata* 38:1–374.
Papike J. J., Taylor L., and Simon S. 1991. Lunar minerals. In *Lunar sourcebook, a user's guide to the Moon*, edited by Heiken G. H., Vaniman D. T. and French B. M. Cambridge, UK: Cambridge University Press. pp. 121–181.
Parashar K., Prasad M. S., and Chauhan S. S. S. 2010. Investigations on a large collection of cosmic dust from the Central Indian Ocean. *Earth Moon Planets* 107:197–217.
Ramdohr P. 1967. Die Schmelzkruste der Meteoriten. *Earth and Planetary Science Letters* 2:197–209.
Roeder P. L. 1994. Chromite: From the fiery rain of chondrules to the Kilauea Iki Lava lake. *The Canadian Mineralogist* 32:729–746.
Schmitz B. 2013. Extraterrestrial spinels and the astronomical perspective on Earth's geological record and evolution of life. *Chemie der Erde-Geochemistry* 73:117–145.
Schmitz B. and Häggström T. 2006. Extraterrestrial chromite in Middle Ordovician marine limestone at Kinnekulle, southern Sweden—Traces of a major asteroid breakup event. *Meteoritics & Planetary Science* 41:455–466.
Schmitz B., Peucker-Ehrenbrink B., Lindström M., and Tassinari M. 1997. Accretion rates of meteorites and cosmic dust in the Early Ordovician. *Science* 278:88–90.
Schmitz B., Tassinari M., and Peucker-Ehrenbrink B. 2001. A rain of ordinary chondritic meteorites in the early Ordovician. *Earth and Planetary Science Letters* 194:1–15.
Schmitz B., Häggström T., and Tassinari M. 2003. Sediment-dispersed extraterrestrial chromite traces a major asteroid disruption event. *Science* 300:961–964.
Schmitz B., Harper D. A. T., Peucker-Ehrenbrink B., Stouge S., Alwmark C., Cronholm A., Bergström S. M., Tassinari M., and Xiaofeng W. 2008. Asteroid breakup linked to the Great Ordovician Biodiversification Event. *Nature Geoscience* 1:49–53.
Schmitz B., Yin Q. Z., Sanborn M. E., Tassinari M., Caplan C. E., and Huss G. R. 2016. A new type of solar-system material recovered from Ordovician marine limestone. *Nature Communications* 7:1–7.

Schmitz B., Heck P. R., Alvarez W., Kita N. T., Rout S. S., Cronholm A., Defouilloy C., Martin E., Smit J., and Terfelt F. 2017. The meteorite flux to Earth in the Early Cretaceous as reconstructed from sediment-dispersed extraterrestrial spinels. *Geology* 45:807–810.

Schönlaub H. P. and Histon K. 2000. The Palaeozoic evolution of the Southern Alps. *Mitteilungen der Oesterreichischen Geologischen Gesellschaft* 92:15–34.

Spoto F., Milani A., and Knezevic Z. 2015. Asteroid family ages. *Icarus* 257:275–289.

Swindle T. D., Kring D. A., and Weirich J. R. 2014. $^{40}Ar/^{39}Ar$ ages of impacts involving ordinary chondrite meteorites. In *Advances in $^{40}Ar/^{39}Ar$ dating: From archeology to planetary sciences*, edited by Jourdan F., Mark D. F., and Verati C. *The Geological Society of London, Special Publications* 378:333–347.

Thorslund P., Wickman F. E., and Nyström J. O. 1984. The Ordovician chondrite from Brunflo, central Sweden, I. General description and primary minerals. *Lithos* 17:87–100.

Torsvik T. H., Smethurst M. A., Van der Voo R., Trench A., Abrahamsen N., and Halvorsen E. 1992. Baltica. A synopsis of Vendian-Permian palaeomagnetic data and their palaeotectonic implications. *Earth-Science Reviews* 33:133–152.

Vokrouhlický D., Brož M., Bottke W. F., Nesvorný D., and Morbidelli A. 2006. Yarkovsky/YORP chronology of asteroid families. *Icarus* 182:118–142.

Walliser O. H. 1964. Conodonten des Silurs. *Abhandlungen des Hessischen Landesamtes für Bodenforschung Wiesbaden* 41:1–106.

Wlotzka F. 2005. Cr spinel and chromite as petrogenetic indicators in ordinary chondrites: Equilibration temperatures of petrologic types 3.7 to 6. *Meteoritics & Planetary Science* 40:1673–1702.

SUPPORTING INFORMATION

Additional supporting information may be found in the online version of this article:

Table S1. Summary of results of elemental analyses of spinel grains from Killeröd and Cellon sections.